Heat-Transfer and Friction Characteristics for the Louver-Fin Heat Exchanger

Joung Ha Kim*
Hanyang University, Seoul 133-791, Republic of Korea
Jae Ho Yun†
Korea Institute of Industrial Technology, Choogchung nam-do 330-825, Republic of Korea
and
Chang Sik Lee‡
Hanyang University, Seoul 133-791, Republic of Korea

The present work focuses on the effects of heat-transfer and friction characteristics for the brazed aluminum louver-fin heat exchanger used in a air conditioner with a relatively low air velocity. The heat-transfer and friction characteristics were experimentally studied for the different louver angles and fin pitches of the louver-fin heat exchanger, which are supposed to be the important parameters. Test conditions were varied by four louver angles, three fin pitches, and various Reynolds numbers of air, which ranged from 110 to 800. The experimental results show that the heat transfer is mainly affected by the fin pitch rather than the louver angle, whereas the pressure drop is affected by the louver angle rather than fin pitch. The performance evaluation criterion of heat exchangers is adopted so that the major operational variables, such as heat-transfer coefficient and pumping power, can be considered simultaneously. The $j/f^{1/3}$ ratios decrease as the louver angle increases. The optimal value of the $j/f^{1/3}$ ratio exists around 20–25 deg of the louver angle. For relatively high louver angles such as 30 and 35 deg, the $j/f^{1/3}$ ratios have almost the same value under the condition that the $Lp/Fp = 1.03, 1.20,$ and 1.43.

Nomenclature

A	=	total surface area, m^2
A_e	=	minimum free flow area, m^2
A_f	=	fin surface area, m^2
A_i	=	inside heat-transfer area, m^2
A_o	=	total heat-transfer area, m^2
A_t	=	external tube surface area, m^2
A_w	=	internal web surface area, m^2
c_p	=	specific heat at constant pressure, J/kg · K
D_h	=	hydraulic diameter of fin array, $D_h = 4A_e F_d/A_o$, mm
F_d	=	depth of fin array in flow direction, mm
F_p	=	fin pitch, mm
F_{th}	=	fin thickness, mm
f	=	friction factor
f_i	=	tube-inlet pressure drop coefficient
H	=	fin height, mm
h_i	=	tube-inside heat-transfer coefficient, W/m^2 · K
h_o	=	tube-outside heat-transfer coefficient, W/m^2 · K
j	=	Colburn factor
K_c	=	abrupt contraction coefficient
K_e	=	abrupt expansion coefficient
k	=	thermal conductivity, W/m · K
L_p	=	louver pitch, mm
l	=	fin length, mm
$\dot{m}$	=	mass flow rate, kg/s
NTU	=	number of heat-transfer units, $UA/c_p W_{min}$
P	=	pumping power, W
Pr	=	Prandtl number
$\dot{Q}$	=	total heat-transfer rate, W
Re_{Lp}	=	Reynolds number based on louver pitch, $Re_{Lp} = \rho u D_h/\mu$
T_p	=	tube pitch, mm
T_w	=	tube width, mm
UA	=	overall thermal conductance, W/K
u	=	air velocity, m/s
V	=	air velocity, m/s
V_c	=	maximum velocity in the core of the heat exchanger, m/s
$1/n$	=	ratio of prototype model to the scale-up model
ΔT	=	temperature difference, K
δ	=	thickness of the tube wall or fin, mm
ε	=	heat-exchanger thermal effectiveness
η	=	overall surface effectiveness of the louver fins
η_f	=	fin efficiency
θ	=	Louver angle, deg
μ	=	dynamic viscosity at mean air temperature, kg/m · s
ρ	=	density of fluid, kg/m^3
ρ_m	=	density of fluid at mean air temperature, kg/m^3
σ	=	contraction ratio of the fin array

Subscripts

a	=	air side
av	=	average value
f	=	fin
i	=	water side
m	=	scale-up model
p	=	prototype model
s	=	standard condition
t	=	wall of the tube
1	=	inlet for air side
2	=	outlet for air side

*Graduate Student, Graduate School, 17 Heangdang-dong, Sungdong-ku.
†Principal Researcher, Advanced Energy and Environment Research Team, 35-3, Hongchon-ri, Ibjang-myun, Chonan-si; jhyun@kitech.re.kr.
‡Professor, Department of Mechanical Engineering, 17 Heangdang-dong, Sungdong-ku.

Introduction

HEAT exchangers are widely used for refrigerators, air conditioners, fan heaters, and automotive and aircraft air-cooling systems. Usually, these kinds of heat exchangers are designed to enhance heat-transfer performance. In general, it is known that thermal

resistance of the air side can be as much as 80% of total thermal resistance. Therefore, for improving performance of heat exchangers it is inevitably necessary to enhance the air-side heat-transfer coefficient. Extended and interrupted fin surfaces have been used to reduce the thermal resistance. The former can improve heat transfer through the increase of surface area, and the latter can reduce the thermal resistance by cutting the thermal boundary layer; these kinds of researches have been conducted by Webb and Trauger[1] and Yun et al.[2]

The louver-fin heat exchanger with peculiar heat-transfer performance was known by Kays and London,[3] who generated the first reliable data on louver surface. Davenport[4] developed an empirical power law correlation by experimental data on 32 louver samples. However, the fin pitches studied by Davenport were much larger than those used in the heat exchanger now, and unconventional fin geometry was tested. Kays and London[5] reported heat-transfer and pressure-drop data on inclined louver fins, but fin spacing was much greater than that used in the present heat exchanger. Achaichia and Cowell[6] provided a correlation to present the performance data for flat-tube and louver-plate fin surfaces. Webb and Jung[7] suggested the significant advantages of a flat tube over a round tube, that is, a lower profile drag, higher fin efficiency, and a low wake region behind the tube. They tested six sample cores and compared their test results with plain plate-fin and spine-fin geometry on round tube. Cowell et al.[8] compared several louver fins and gave designers effective information for offset or louver fins considering the importance of size, weight, and pumping power for the application. Chang and Wang[9] provided data on 27 samples of louver-fin heat exchangers with the different geometrical parameters such as tube width, louver length, louver pitch, fin height, and fin pitch.

DeJong and Jacobi[10,11] visualized a flow pattern through large arrays of plates with naphthalene sublimation technique. From the flow-visualization results these local data revealed the effects of boundary-layer growth and vortex shedding in the array. And they have shown that flow near wall is characterized by lower flow efficiency, large separation and recirculation zones between louvers, and a transition to unsteady flow at lower Reynolds numbers. Also, the effect of shape of fin exchanger on the air-side performance is investigated under dry and wet conditions by Kim et al.[12] For the dry and wet surface condition they reported that the heat-transfer performance was neither influenced significantly by the inclination angle (-60 deg $< \theta < 60$ deg), nor by the presence or absence of an upstream duct, while the pressure drops increased consistently with the inclination angle.

Although many researchers have reviewed various experimental studies for brazed aluminum louver-fin heat exchanger, the papers for the relatively high louver angle and low fin pitch have been rarely reported. In this case fan power for compact louver-fin heat exchangers has become the important factor. In this study double-enlarged louver-fin heat exchangers are investigated for different louver angle and louver pitch. To obtain the effects of performance parameters on the heat-transfer and friction characteristics of the louver-fin heat exchanger, the experiments of heat exchanger were performed for the four louver angles and three fin pitches of louver-fin heat exchanger.

Heat-Transfer and Friction Characteristics

Theoretical Analysis of the Scale-Up Model

Scale-up modeling is needed for geometrical similarity and theoretical research that concerns the continuity equations, momentum equations, and energy equations. Wong and Smith[13] demonstrated the airflow phenomena of louver-fin heat exchanger by using the scale-up model, and the characteristics of heat-transfer and flow performance of heat exchanger were investigated by many researchers.[14,15] First of all, the continuity equation and momentum equation can be obtained:

$$\nabla \cdot V = 0 \tag{1}$$

$$(V \cdot \nabla)V = -\nabla P + (1/Re_D)\nabla^2 V \tag{2}$$

Figure 1 shows the louver-fin core geometry. When we apply the scale-up louver-fin heat exchanger to the prototype louver-fin heat exchanger, there is a relation between Reynolds number for the scale-up model and the prototype,

$$(\rho u D_h/\mu)_p = (\rho u D_h/\mu)_m \tag{3}$$

For the sake of reliability, the experimental study of a heat exchanger is conducted for the scale-up model with which the heat-transfer performance and pressure-drop characteristics can be investigated in more detail. Then the same values of density and viscosity for the working fluid are given to the prototype. Therefore, air velocity with the fluid field is reduced to the geometrical similarity ratio of the scale-up model to the prototype model. At the same time it is necessary that the similarity of air temperature be related to the similar relationships of heat transfer. Thus Eq. (4) can be obtained for the energy equation as the function of Reynolds number, Prandtl number, and fin surface temperature.

$$V(\nabla \cdot T) = (1/Re_D Pr)\nabla^2 T \tag{4}$$

where the same value of the Prandtl number can be used for the same fluid. Then similarity of fin surface temperature is derived from fin heat-transfer equation.

$$T_f = f\left[X^*, Y^*, Z^*, (F_{th}/k)\right] \tag{5}$$

where X^*, Y^*, and Z^* are dimensionless length. The k has the same value for the same fin material, and F_{th} is adjusted to a geometrical similarity ratio of the scale-up model to the prototype model. (The ratio of the prototype model to the scale-up model was 1 to n, then the experimental study was applied to $1/n$ of air velocity for the fluid field and similarity relationship of heat transfer.)

Heat Transfer

The average heat-transfer rate of $\dot{Q}_a$ and $\dot{Q}_i$ is given by

$$\dot{Q}_{av} = (\dot{Q}_a + \dot{Q}_i)/2 \tag{6}$$

where the heat-transfer rate of $\dot{Q}_a$ and $\dot{Q}_i$ are written as
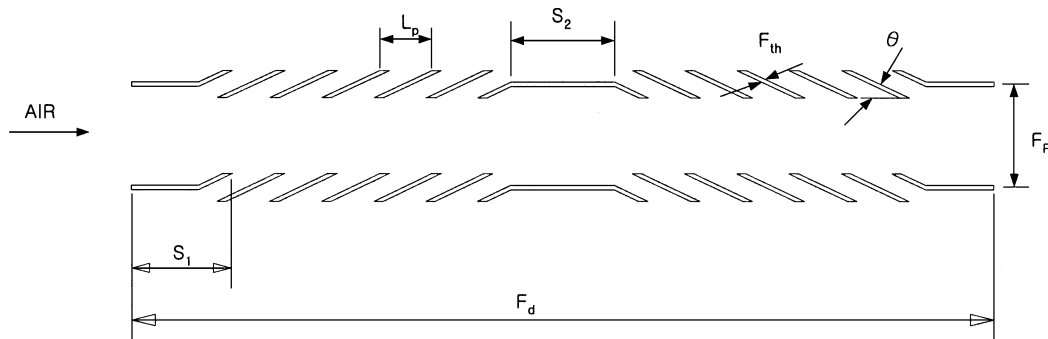
$$\dot{Q}_a = \dot{m}_a c_{pa} \Delta T_a \tag{7}$$

Fig. 1   Louver-fin core geometry.

Table 1 Geometrical parameters of test samples

Samples	L_p, mm	L_l, mm	θ, deg	H, mm	F_p, mm	F_{th}, mm	F_d, mm	T_w, mm	T_p, mm	L_p/F_p	No. of fin/ 50.8 mm
1	2.9	12.5	20	16.5	2.82	0.15	44	5	21.2	1.03	18
2	2.9	12.5	20	16.5	2.42	0.15	44	5	21.2	1.20	21
3	2.9	12.5	20	16.5	2.03	0.15	44	5	21.2	1.43	25
4	2.9	12.5	25	16.5	2.82	0.15	44	5	21.2	1.03	18
5	2.9	12.5	25	16.5	2.42	0.15	44	5	21.2	1.20	21
6	2.9	12.5	25	16.5	2.03	0.15	44	5	21.2	1.43	25
7	2.9	12.5	30	16.5	2.82	0.15	44	5	21.2	1.03	18
8	2.9	12.5	30	16.5	2.42	0.15	44	5	21.2	1.20	21
9	2.9	12.5	30	16.5	2.03	0.15	44	5	21.2	1.43	25
10	2.9	12.5	35	16.5	2.82	0.15	44	5	21.2	1.03	18
11	2.9	2.42	35	16.5	44	12.5	0.15	5	21.2	1.20	21
12	2.9	2.03	35	16.5	44	12.5	0.15	5	21.2	1.43	25

$$\dot{Q}_i = \dot{m}_i c_{pi} \Delta T_i \qquad (8)$$

Heat-transfer performance can be represented by the j factor[16] obtained from the air-side heat-transfer coefficient. The UA can be calculated using the ε-NTU (effectiveness number of transfer unit) method for unmixed-unmixed crossflow. Assuming zero-water-side fouling resistance, the air-side heat-transfer coefficient was obtained by subtracting the water-side and wall resistances from the total thermal resistance:

$$1/\eta_a h_a A_a = (1/UA) - (1/h_i A_i) - (\delta_t/k_t A_t) \qquad (9)$$

For single-phase fluid within a smooth tube, h_i is calculated from the semi-empirical correlation described by Gnielinski[17]:

$$h_i = \left(\frac{k_i}{D_{h,i}}\right) \frac{(Re_{Dh,i} - 1000) Pr_i (f_i/2)}{1.0 + 12.7(f_i/2)^{0.5}\left(Pr_i^{\frac{2}{3}} - 1\right)} \qquad (10)$$

where f_i given by

$$f_i = [1.58 \, \ell n(Re_{Dh,i}) - 3.28]^{-2} \qquad (11)$$

The fin efficiency for the plate fin surface geometry η_f is calculated by Shah[18]

$$\eta_f = \tanh(ml)/ml \qquad (12)$$

where m and l are given by

$$m = \sqrt{2h_a/k_f \delta_f (1 + \delta_f/F_d)} \qquad (13)$$

$$l = H/2 - \delta_f \qquad (14)$$

η can be calculated from

$$\eta = 1 - A_f/A_a(1 - \eta_f) \qquad (15)$$

Air-side heat-transfer coefficient h_a is calculated from Eq. (9). In this calculation the effective h_a is taken within the value $|h_{a,old} - h_{a,new}| \leq 10^{-5}$. Thus, the j factor can be calculated from air-side heat-transfer coefficient
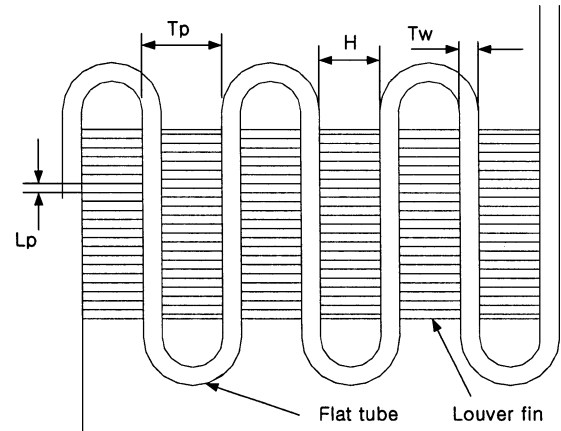
$$j = \frac{h_a}{\rho_m V_c c_{pa}} Pr_a^{\frac{2}{3}} \qquad (16)$$

Pressure Drop

The pressure drop takes place in the airflow through brazed aluminum heat exchanger. The pressure difference is reduced to determine the Fanning friction factor f:

$$f = \frac{A_c}{A} \frac{\rho_m}{\rho_1} \left[\frac{2\rho_1 \Delta P}{(\rho_m V_c)^2} - \left(K_c + 1 - \sigma^2\right) - 2\left(\frac{\rho_1}{\rho_2} - 1\right) \right.$$

$$\left. + \left(1 - \sigma^2 - K_e\right) \frac{\rho_1}{\rho_2} \right] \qquad (17)$$

In Eq. (17) the abrupt contraction and expansion coefficients K_c and K_e are calculated at $Re_{Dh} = \infty$ by Kays and London.[5]

Fig. 2 Schematic diagram of the heat exchanger.

Experimental Apparatus and Test Procedures

Experimental Apparatus

The serpentine flat-tube and brazed aluminum louver-fin heat exchangers are used in this experiment as double scale-up model of reference louver-fin heat exchanger. The test heat exchanger consisted of a six-array fin (thickness of 15 mm) and a seven-pass tube (width of 44 mm, thickness of 0.5 mm). The frontal area of the test samples is 6756.4 mm^2 (width of 133 mm, height of 50.8 mm). The geometrical parameters of this study are louver angles of 20, 25, 30, and 35 deg and fin pitches of 2.82, 2.42, and 2.03 mm. A notational description of the heat exchanger is shown in Fig. 2. Table 1 shows the geometrical parameters of the test samples.

The experimental apparatus is composed of an open-type wind tunnel with an induced fan, constant temperature and humidity chamber, measurement section of air temperature, constant temperature water vessel, magnetic flow meter for water side, and differential pressure transducer as shown in Fig. 3. The wind tunnel is made of acrylic acid resin of 10 mm in thickness.

Experimental Procedures

The airflow rate is controlled by a 0.5-kW centrifugal fan with an inverter. The inlet air of test samples is well mixed by a wire screen of 250×300 mm. The airflow velocity is measured by a hot-film airflow meter calibrated within 0.3% accuracy. The inlet and outlet of test samples are equipped with thermocouple meshes for temperature measurement. That is, the four thermocouples are installed in the inlet thermocouple mesh while the outlet is set up with 12 thermocouples. The differential pressure transducer calibrated within 1 Pa is used for measurement of pressure drop between the inlet and outlet of the sample with each four ports. The water in flat tube is supplied from the constant temperature water vessel. The mass flow rate of water is regulated by a bypass valve. The inlet and outlet water temperatures of the tube side are measured by precalibrated resistance temperature detection sensors within 0.1°C of accuracy. To measure the mass-flow rate, the water-flow rate is detected by
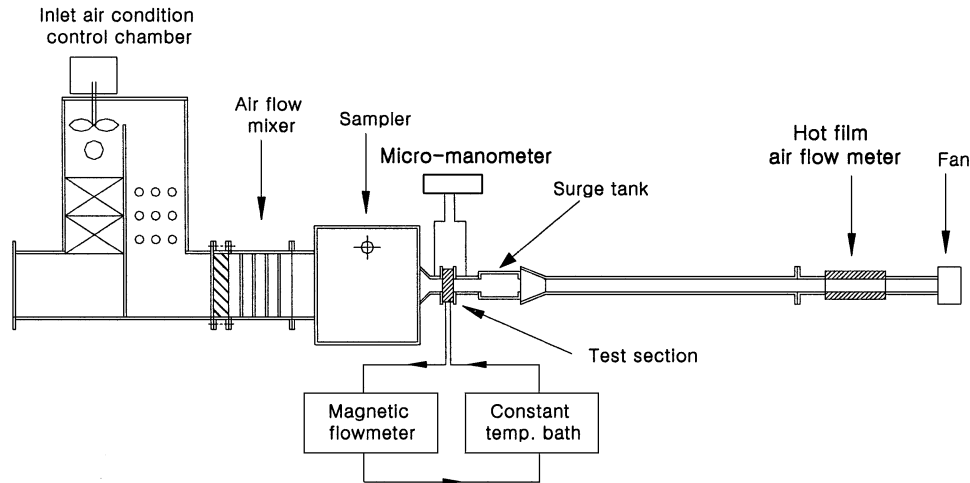
Fig. 3   Schematic of the experimental apparatus.

using a magnetic flow meter. The temperatures of water and air, pressure drop, air velocity, and mass-flow rate of water are collected by a data-acquisition system and transported to the computer through a RS-232C interface-bus.

The experiment was carried out for air velocity with $1 \sim 4$ m/s of a scale-up model and constant temperature $19°C \pm 0.2°C$. The actual air velocity of the prototype model becomes $0.5 \sim 2$ m/s. The mass-flow rate of water was fixed at 0.083 kg/s and $45°C \pm 0.1°C$. In this study the energy balance between air and water side is within $\pm 5\%$.

Results and Discussion

Comparison with Other Studies

The performance of scale-up heat exchangers can be evaluated by the j and f factors calculated from the measured data of air and water inlet and outlet temperature, air velocity, mass-flow rate of water, and pressure drop. The effects of fin angles and fin pitches on the performance of heat-transfer and friction characteristics were investigated by using a louver-fin heat exchanger and experimental apparatus as shown in Figs. 2 and 3.

Using the method suggested by Moffat,[19] uncertainties of this work for the Colburn j factor and friction factor f were calculated. The uncertainties of present investigation are estimated from 2.5 to 4.2% for the j factor and from 3.8 to 5.3% for the f factor.

The j and f factors in this study were compared with correlation equations of Davenport[4] for the f factor, Chang and Wang[9] for the j factor, and Sunden and Svantesson[20] for the j factor. Figure 4 shows the comparison of the f factors of the Davenport's correlation with experimental results of this work for louver-fin heat exchanger at louver angle, 20 deg and Lp/Fp, 1.03. As shown in the figure, the tendency of the f factors describes the same trend for the range of Reynolds number Re_{Lp} from 250 to 1000, but the results bring about difference from the Davenport's correlation for the range of Reynolds number Re_{Lp} under 200. It also shows that the j factors in the experimental data agreed with correlation equations of Chang and Wang[9] for the j factors with Re_{Lp} under 250 and correlation equations of Sunden and Svantesson[20] for the j factors with Re_{Lp} over 250.

Effects of the Lp/Fp Ratio

The Colburn j factor and friction factor f of the louver-fin heat exchanger are described in Figs. 5–8 for Reynolds number Re_{Lp} based on louver pitch. As shown in Figs. 5 and 6, the influences of the Lp/Fp ratio on the heat transfer and friction decrease with the increase of Reynolds number Re_{Lp} at most of the degrees of the louver angle. But there is exception for the j factors on Fig. 5. Namely, the airflow efficiency increases as Lp/Fp and louver angles decrease within the range of Reynolds numbers from 110 to 800, whereas for the relatively high Reynolds number the j factors
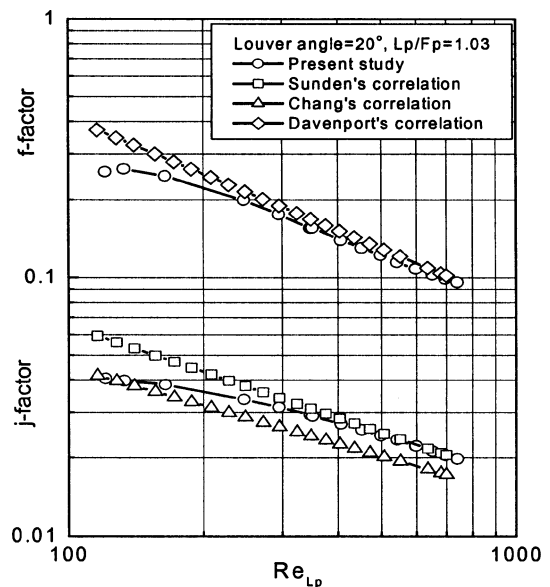

Fig. 4   Correlation between the j factor and the f factor for the Reynolds number of the louver fin.

increase with high Lp/Fp because the airflow efficiency is enhanced. As the value of the Lp/Fp ratio increases, the j factors decrease, but f factors increase at low Reynolds numbers. However, as the Reynolds number Re_{Lp} increases, the j factors become saturated for all of the values of the Lp/Fp. In other words, the airflow efficiency is almost the same with all of the values of the Lp/Fp over 1.03 and has a little influence on the j factors.

The characteristics of the j factors and f factors show the same trends as shown in Figs. 7 and 8. As the Lp/Fp increases for the fixed value of louver pitch, the fin spacing and the friction factor f increase by the increase of frictional resistance. But the f factor is less affected by the Lp/Fp than the louver angle and has almost the same value for the Lp/Fp at the relatively high louver angles, as shown in Fig. 8. That is, for a high-louver-angle flow resistance becomes much larger than frictional resistance that increases as the fin surface increases. This result shows that the low value of Lp/Fp can be used at a low Reynolds number when a louver fin is designed.

Effects of Louver Angle

The major operational variables of heat exchanger include the heat-transfer rate, the pumping power, the fluid velocity, and the heat-exchanger flow rate. These are deeply concerned with the performance evaluation criterion of design constraints for the heat
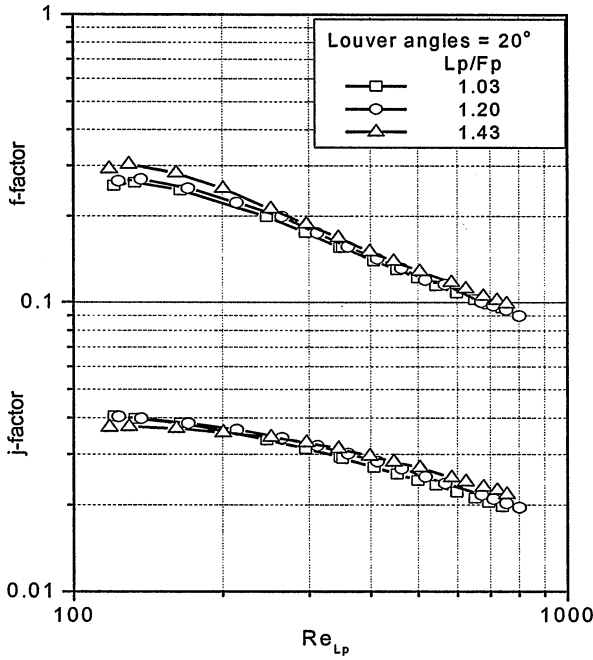
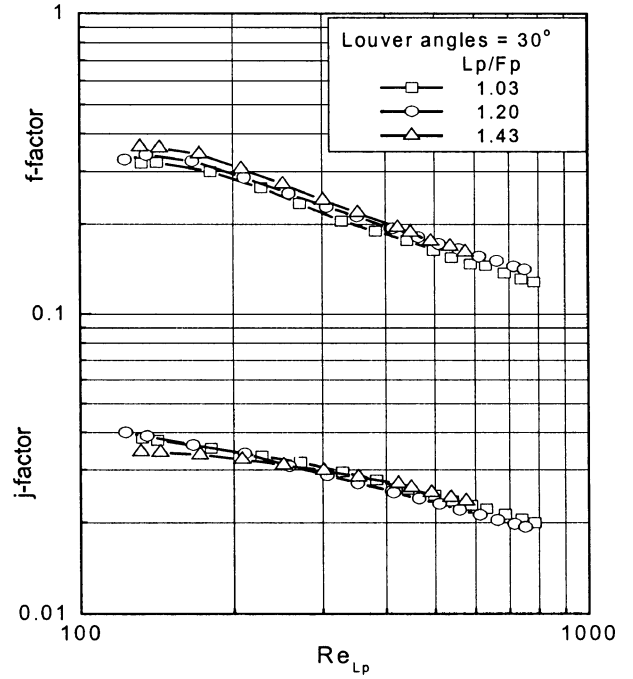**Fig. 5   Influences of *Lp/Fp* on the *j* factor and *f* factor (louver angle = 20 deg).**

Fig. 7   Influences of *Lp/Fp* on the *j* factor and *f* factor (louver angle = 30 deg).

Fig. 6   Influences of *Lp/Fp* on the *j* factor and *f* factor (louver angle = 25 deg).
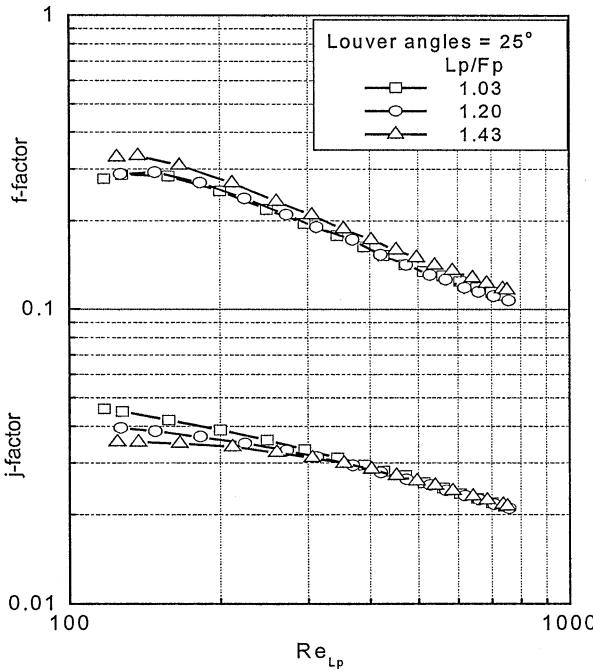

Fig. 8   Influences of *Lp/Fp* on the *j* factor and *f* factor (louver angle = 35 deg).

exchangers. Webb[21] described a performance evaluation criterion of heat exchanger as Eq. (18).

$$\frac{hA/h_s A_s}{(P/P_s)^{\frac{1}{3}}(A/A_s)^{\frac{2}{3}}} = \frac{j/j_s}{(f/f_s)^{\frac{1}{3}}} \qquad (18)$$

Equations (19) and (20) can be substituted for the Eq. (16) of the *j* factor and for Eq. (17) of the *f* factor:

$$\frac{hA}{h_s A_s} = \frac{jA\rho_m V_c}{j_s A_s \rho_{ms} V_{cs}} \qquad (19)$$

$$\frac{P}{P_s} = \frac{fA\rho_m V_c}{f_s A_s \rho_{ms} V_{cs}} \qquad (20)$$

Equation (18) can be calculated from elimination of the term $\rho_m V_c/\rho_{ms}V_{cs}$ with Eqs. (19) and (20). Every standard value is set by constant values of this study, and the variables on the right-hand side of Eq. (18) are induced by the $j/f^{1/3}$.

The ratios of the *j* factors to the $f^{1/3}$ factors against Reynolds number Re_{Lp} can be viewed as the better merit of effect for heat transfer to the pressure drop in Figs. 9–11. Thus, the higher $j/f^{1/3}$ ratios describe better performance of heat transfer to the pressure drop.

Figure 9 shows the effect of louver angle on the $j/f^{1/3}$ ratios at 1.03 of the Lp/Fp. As shown in the comparison of the $j/f^{1/3}$ ratios, the louver angles have the significant influence on the $j/f^{1/3}$ ratios. The $j/f^{1/3}$ ratios decrease as the louver angle increases because a high louver angle becomes the large obstacle for the airflow and the *f* factors for the high louver angles are larger than those for the low
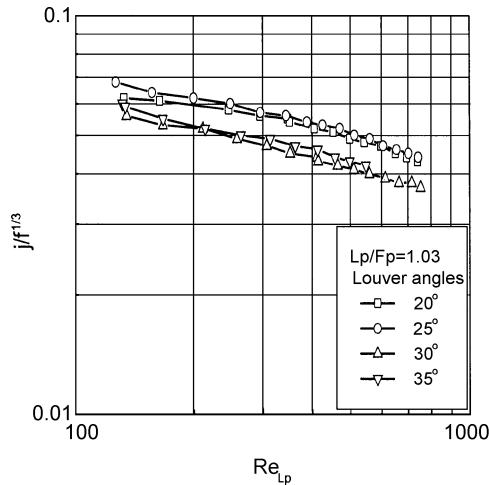
Fig. 9   Influences of louver angles on the $j/f^{1/3}$ ratios ($Lp/Fp = 1.03$).
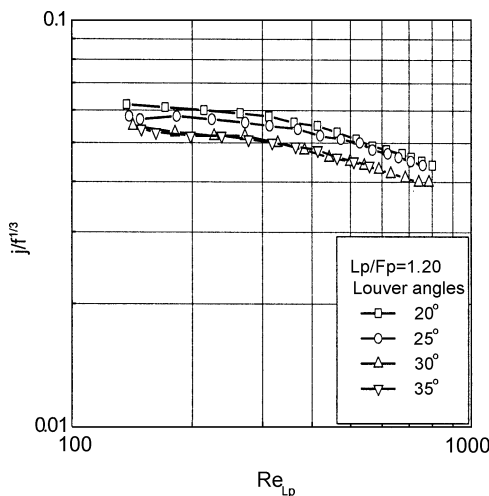

Fig. 10   Influences of louver angles on the $j/f^{1/3}$ ratios ($Lp/Fp = 1.20$).
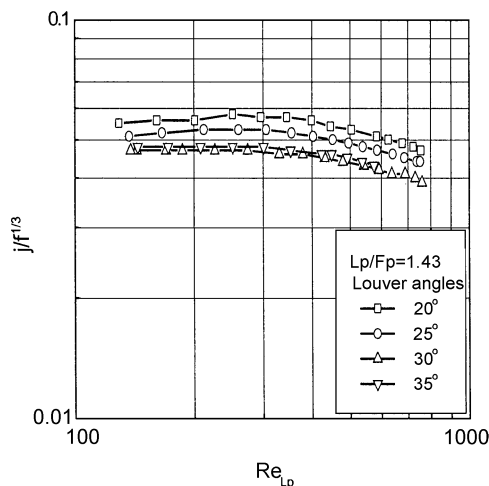

Fig. 11   Influences of louver angles on the $j/f^{1/3}$ ratios ($Lp/Fp = 1.43$).

louver angles. For this reason, the $j/f^{1/3}$ ratio has the highest value with 25 deg of louver angle.

Figures 10 and 11 show the effects of louver angles and louver-fin pitches on the $j/f^{1/3}$ ratio of louver-fin heat exchangers. The characteristics of the $j/f^{1/3}$ ratios describe almost the same trends for the louver angles as shown in Fig. 9, but the $j/f^{1/3}$ ratios of Figs. 10 and 11, in which the Lp/Fp are relatively high, that is, 1.20 to 1.49, have the highest value with 20 deg of louver angle. As illustrated in these Figs. 9–11 for 30 and 35 deg of louver angle, the

$j/f^{1/3}$ ratios have almost the same values at the conditions of the $Lp/Fp = 1.03$, 1.20, and 1.43.

The thermal and flow boundary layer are concerned with airflow profile that is mainly influenced by louver angle and Lp/Fp. The higher louver angle has the longer airflow path. Consequently, this effect gave rise to the higher pressure drop but has a little influence on the heat transfer. As can be seen in Figs. 9–11, the optimal value of the $j/f^{1/3}$ ratios exists around $20 \sim 25$ deg of louver angle.

Conclusions

The performance of heat-transfer and friction characteristics were investigated for the various louver angles and the Lp/Fp of the louver-fin heat exchanger. Based on the experimental results, the conclusions of this study are as follows:

1) The performances of heat-transfer and friction characteristics were compared with the correlation equations of Davenport[4] for the f factor, Chang and Wang[9] for the j factor, and Sunden and Svantesson[20] for the j factor. The f factors and j factors in this study well agreed with Davenport's correlation and Sunden and Svantessen's correlation, respectively.

2) The friction factors are highly increased with the increase of the louver angle, and these values are a little influenced by the variation of the Lp/Fp as the louver angle increases.

3) The $j/f^{1/3}$ ratios decrease as the louver angle increases. The optimal value of the $j/f^{1/3}$ ratio exists around 20–25 deg of the louver angle.

4) For relatively high louver angles such as 30 and 35 deg, the $j/f^{1/3}$ ratios have almost the same values under the condition that the Lp/Fp are 1.03, 1.20, and 1.43.

References

[1]Webb, R. L., and Trauger, P., "The Flow Structure in the Louvered Fin Feat Exchanger Geometry," *Experimental Thermal and Fluid Science*, Vol. 4, No. 2, 1991, pp. 204–217.

[2]Yun, J. H., Kim, J. H., Lee, C. H., and Pack, J. H., "An Experimental Study in the Heat Transfer and Friction Characteristics in the Louvered-Fin for Flat-Tube Heat Exchanger," *Proceedings of the SAREK '97 Winter Annual Conference*, Society of Air-Conditioning and Refrigerating Engineers of Korea, Seoul, Korea, 1997, pp. 171–176.

[3]Kays, W. M., and London, A. L., "Heat Transfer and Flow Friction Characteristics of Some Compact Heat Exchanger Surface," *Transactions of the ASME*, Vol. 72, Nov. 1950, pp. 1075–1085.

[4]Davenport, C. J., "Correlation for Heat Transfer and Flow Friction Characteristics of Louvered Fin," *Heat Transfer-Seattle*, edited by N. M. Farukhi, AIChE Symposium, Vol. 79, No. 225, 1983, pp. 19–27.

[5]Kays, W. M., and London, A. L., *Compact Heat Exchangers*, 3rd ed, McGraw–Hill, New York, 1984, pp. 234–241.

[6]Achaichia, A., and Cowell, T. A., "Heat Transfer and Pressure Drop Characteristics of Flat Tube and Louvered Plate Fin Surfaces," *Experimental Thermal and Fluid Science*, Vol. 1, No. 2, 1988, pp. 147–157.

[7]Webb, R. L., and Jung, S. H., "Air-Side Performance of Enhanced Brazed Aluminum Heat Exchangers," *ASHRAE Transactions*, Vol. 98, No. 2, 1992, pp. 391–401.

[8]Cowell, T. A., Heikal, M. R., and Achaichia, A., "Flow and Heat Transfer in Compact Louvered Fin Surface," *Experimental Thermal and Fluid Science*, Vol. 10, No. 2, 1993, pp. 192–199.

[9]Chang, Y. J., and Wang, C. C., "Air Side Performance of Brazed Aluminum Heat Exchanger," *Journal of Enhanced Heat Transfer*, Vol. 3, No. 1, 1996, pp. 15–28.

[10]DeJong, N. C., and Jacobi, A. M., "An Experimental Study of Flow and Heat Transfer in Parallel-Plate Arrays: Local, Row-by-Row and Surface Average Behavior," *International Journal of Heat and Mass Transfer*, Vol. 40, No. 6, 1997, pp. 1365–1378.

[11]DeJong, N. C., and Jacobi, A. M., "Flow, Heat Transfer, and Pressure Drop in the Near-Well Region of Louvered-Fin Array," *Experimental Thermal and Fluid Science*, Vol. 27, No. 3, 2003, pp. 237–250.

[12]Kim, M. H., Youn, B., and Bullard, C. W., "Effect of Inclination on the Air-Side Performance of a Brazed Aluminum Heat Exchanger Under Dry and Wet Conditions," *International Journal of Heat and Mass Transfer*, Vol. 44, No. 24, 2001, pp. 4613–4623.

[13]Wong, L. T., and Smith, M. C., "Air Flow Phenomena in the Louvered Fin Heat Exchanger," Society of Automotive Engineers, Paper 730237, Jan. 1973.

[14]Yun, J. Y., and Lee, K. S., "Investigation of Heat Transfer Characteristics on Various Kinds of Fin-and-Tube Heat Exchangers with Interrupted

Surfaces," *International Journal of Heat and Mass Transfer*, Vol. 42, No. 13, 1999, pp. 2375–2385.

[15]Torikoe, K., Kawabata, K., and Kawazoe, M., "Heat Transfer Characteristics on Fin-and-Tube Type Heat Exchanger," *Proceedings of the 27th JAP Annual Conference*, Japanese Assoc. of Refrigeration, Tokyo, Japan, 1993, pp. 109–112.

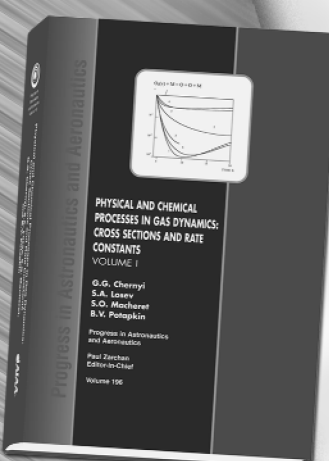[16]Colburn, A. P., "A Method of Correlating Forced Convection Heat Transfer Data and a Comparison with Fluid Friction," *Transactions of the AIChE*, Vol. 29, 1933, pp. 174–210.

[17]Gnielinski, V., "New Equation for Heat and Mass Transfer in Turbulent Pipe and Channel Flow," *International Chemical Engineering*, Vol. 16, No. 2, 1976, pp. 359–368.

[18]Shah, R. K., "Compact Heat Exchangers," Handbook of Heat Transfer Applications, 2nd ed., edited by W. M. Rohsenow, J. P. Hartnett, and E. N. Ganic, McGraw–Hill, New York, 1985, pp. 181–200.

[19]Moffat, R. J., "Describing the Uncertainties in Experimental Results," *Experimental Thermal and Fluid Science*, Vol. 1, No. 1, 1988, pp. 3–17.

[20]Sunden, B., and Svantesson, J., "Correlations of j- and f-factors for Multilouvered Heat Transfer Surfaces," *Proceedings of the 3rd United Kingdom National Heat Transfer Conference*, No. 129, Inst. of Chemical Engineers, Birmingham, UK, 1992, pp. 805–811.

[21]Webb, R. L., *Principles of Enhanced Heat Transfer*, Wiley, New York, 1994, pp. 56–73.